Dependence of the Conformational Isomerism in 1-n-Butyl-3-methylimidazolium Ionic Liquids on the Nature of the Halide Anion

ARTICLE *in* THE JOURNAL OF PHYSICAL CHEMISTRY B · SEPTEMBER 2010

Impact Factor: 3.3 · DOI: 10.1021/jp1044755 · Source: PubMed

10 AUTHORS, INCLUDING:

Jose Nuno A Canongia Lopes
Technical University of Lisbon
179 PUBLICATIONS **8,313** CITATIONS
SEE PROFILE

Agílio A H Pádua
Université Blaise Pascal - Clermont-Ferrand II
210 PUBLICATIONS **5,962** CITATIONS
SEE PROFILE

Shinji Kohara
Japan Synchrotron Radiation Research Ins…
247 PUBLICATIONS **2,454** CITATIONS
SEE PROFILE

Kenta Fujii
Yamaguchi University
83 PUBLICATIONS **1,752** CITATIONS
SEE PROFILE

Dependence of the Conformational Isomerism in 1-*n*-Butyl-3-methylimidazolium Ionic Liquids on the Nature of the Halide Anion

Yasuhiro Umebayashi,*,† Hiroshi Hamano,† Seiji Tsuzuki,*,‡ José N. Canongia Lopes,§ Agilio A. H. Pádua,|| Yasuo Kameda,⊥ Shinji Kohara,# Taishi Yamaguchi,† Kenta Fujii,▽ and Shin-ichi Ishiguro†

Department of Chemistry, Faculty of Science, Kyushu University, Hakozaki, Higashi-ku, Fukuoka 812-8581, Japan, National Institute of Advanced Industrial Science and Technology (AIST), Tsukuba Center 5, Tsukuba, Ibaraki 305-8565, Japan, Centro de Química Estrutural, Instituto Superior Técnico, 1049 001 Lisboa, and Instituto de Tecnologia Química e Biológica, UNL, Av. República Ap. 127, 2780 901 Oeiras, Portugal, Laboratoire Thermodynamique et Interactions Moléculaires, Université Blaise Pascal Clermont-Ferrand and CNRS UMR6272, France, Department of Material and Biological Chemistry, Faculty of Science, Yamagata University, Kojirakawa-machi 1-4-12, Yamagata 990-8560, Japan, Japan Synchrotron Radiation Research Institute (JASRI), Sayo-cho, Sayo-gun, Hyogo 679-5198, Japan, and Neutron Science Labolatory, Institute for Solid State Physics, The University of Tokyo, Kashiwa, Chiba 277-8581, Japan

Received: May 17, 2010; Revised Manuscript Received: July 24, 2010

The conformational isomerism of the 1-*n*-butyl-3-methylimidazolium cation, $[C_4mim]^+$, in halide-based ionic liquids—[C_4mim]Cl, [C_4mim]Br, and [C_4mim]I—was explored by Raman spectroscopy. The $[C_4mim]^+$ cation exhibits *trans*−*gauche* conformational isomerism with respect to the N1−C7−C8−C9 dihedral angle of its butyl chain. The thermodynamics of *trans*−*gauche* conversion were analyzed through the successful evaluation of the corresponding Gibbs free energy, $\Delta_{iso}G°$, enthalpy, $\Delta_{iso}H°$, and entropy, $\Delta_{iso}S°$, of conformational isomerization. The values of $\Delta_{iso}G°$ obtained are small (a few units of kJ/mol) and show a slight negative variation with the decrease of the size of the halide anion. On the other hand, $\Delta_{iso}H°$ and $\Delta_{iso}S°$ values are positive for [C_4mim]I and decrease with the anion size to yield negative values for [C_4mim]Cl and [C_4mim]Br. This suggests that the negative electrostatic field around the halide anions stabilizes the *gauche* isomer from an enthalpic point of view. In order to study the structure and ion−ion interactions in this type of ionic liquids, high-energy X-ray diffraction experiments were performed for [C_4mim]Cl at different temperatures and for supercooled [C_4mim][Br] at ambient temperature. Molecular dynamics (MD) simulations for these systems were also carried out at several temperatures. $\Delta_{iso}G°$ and $\Delta_{iso}H°$ values derived from the simulations qualitatively agree with the experimental ones. Experimental X-ray structure factors are also well reproduced by the simulations. The MD results also allowed the calculation of different spatial distribution functions (SDFs) for the three ionic liquids. Although all SDFs exhibit similar trends, [C_4mim]I shows a reduced anion density facing the C_2−H atoms of the cation and enhanced anion densities above and below the imidazolium ring plane. This indicates that anions localized near the C_2−H atoms of the cation can stabilize their *gauche* conformer, an effect that is stronger with smaller anions. This conclusion is also supported by ab initio calculations at the CCSD(T) level for isolated ion pairs.

Introduction

Room-temperature ionic liquids are expected to be good alternatives to common nonaqueous solvents in a wide range of chemical applications due to their distinctive and valuable properties such as almost null volatility or nonflammability.[1–3] From a physical chemistry point of view, the molecular origin of such unique properties is quite interesting and defines a new class of condensed matter.[4–7] At a molecular level, the flexibility of the molecular structure of ionic liquids is one of the key features needed to understand their macroscopic physicochemical properties.

Endo et al. have shown that 1-*n*-butyl-3-methylimidazolium hexafluorophosphate, [C_4mim][PF_6], has three crystalline phases and that all its phase transitions, except the glass transition, are associated with conformational changes of the butyl group.[8] Similar behavior has been found for other ionic liquids.[8–13] Moreover, Blokhin and Paulechka have studied the polymorphism of 1-alkyl-3-methylimidazolium bis(trifluoromethanesulfonyl) amide, [$C_n$mim][TFSA].[14–17] Thus, conformational isomerism of the $[C_nmim]^+$ cation is considered to play a key role in solid/liquid phase transition processes of ionic liquids and is a well studied and reviewed line of research.[18,19]

Chart 1 shows the molecular structures of three possible conformational isomers of $[C_4mim]^+$ optimized at the B3LYP/6-311+G(d,p) level of theory. The $[C_4mim]^+$ cation has *trans*−*gauche* conformational isomerism with respect to the N1−C7−C8−C9 and the C7−C8−C9−C10 dihedral angles,

* To whom correspondence should be addressed. E-mail: yumeb@chem.kyushu-univ.jp (Y.U.); s.tsuzuki@aist.go.jp (S.T.). Phone and fax: +81-92-642-2582 (Y.U.).

† Kyushu University.

‡ National Institute of Advanced Industrial Science and Technology (AIST.

§ Instituto Superior Técnico and Instituto de Tecnologia Química e Biológica, UNL.

|| Université Blaise Pascal Clermont-Ferrand and CNRS UMR6272.

⊥ Yamagata University.

Japan Synchrotron Radiation Research Institute (JASRI).

▽ The University of Tokyo.

10.1021/jp1044755
Published on Web 08/19/2010

CHART 1: Illustrative Molecular Structures of 1-*n*-Butyl-3-methylimidazolium (C_4mIm^+) and Optimized Geometries for the Respective Conformational Isomers of *TT*, *GT*, and *G′T* at the B3LYP/6-311+G(d,p) Level Calculations

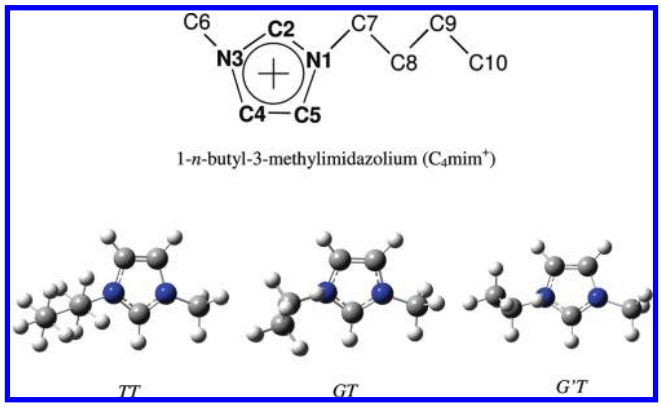

yielding *TT* and *GT* isomers, respectively. These were first experimentally observed as polymorphs of the corresponding halide crystals.[20–23] Later, Katayanagi et al. clearly demonstrated that the conformational isomerism in the liquid state depends on the halide counterion, i.e., the concentration of the *GT* isomer increases remarkably for smaller halide ions.[24] Berg et al. explored this fact in detail by means of Raman spectroscopy and ab initio calculations,[25] and several other researchers have applied similar techniques to reveal the conformational isomerism of the $[C_4mim]^+$ cation.[26–30] In addition, Chang et al. demonstrated by means of high-pressure Raman spectroscopy that high-pressure phases arise from the perturbed *GT* conformer, that the *GT* conformer population decreases with increasing pressure, and that the *GT* and *TT* conformers of [C_4mim]Br and [C_4mim]Cl crystals, respectively, are thermodynamically more stable at ambient pressure.[31,32] On the other hand, although molecular simulations are being used intensively for studying structural and dynamic aspects of ionic liquids,[33–68] only a few studies have addressed the issue of conformational isomerism of the $[C_4mim]^+$ cation.[69–71] According to some of those investigations, the populations of the isomers with N1−C7−C8−C9 dihedral angles of 180° (*T* isomer) are smaller than those with dihedral angles of 60° (*G* isomer) in [C_4mim]-based ionic liquids of tetrafluoroborate, $[BF_4]^-$, hexafluorophosphate, $[PF_6]^-$, and bis(trifluoromethanesulfonyl)amide, $[TFSA]^-$, and the population ratio of the two isomers is almost independent of the counteranion.[71] In fact, the anion effect on the conformational isomerism equilibria of $[C_4mim]^+$ in the liquid state has not been clearly analyzed.

Such an effect is caused by the self-solvation that ionic liquids experience in the condensed phase and how this affects the torsion potential energy surface of a given dihedral angle; i.e., the geometry of a given $[C_4mim]^+$ conformer is stabilized by the presence and spatial arrangement of surrounding anions whose position is in turn defined by the self-solvation of cation−anion interactions. Therefore, in order to understand the conformational isomerism of the butyl chain of $[C_4mim]^+$ in ionic liquids, it is indispensable to examine the cation−anion interactions. In the gas phase, those have been investigated by ab initio calculations.[72–77] In addition, the closest-neighbor cation−anion orientations and configurations in the condensed phase of ionic liquids were elucidated experimentally.[24,78–88] Recently, we have reported the liquid structure and the first-shell cation−anion interactions in several ionic liquids by means of large angle X-ray scattering (LAXS)[89–93] and high-energy X-ray diffraction (HEXRD) techniques[94] with the aid of MD simulation. This powerful combination of experimental and MD simulation techniques can provide useful information on the cation−anion interactions and also structural information such as orientation and configuration in ionic liquids at an atomistic level.

In this paper, we used Raman spectroscopy to determine for the first time several thermodynamic properties—Gibbs free energy, $\Delta_{iso}G°$, enthalpy, $\Delta_{iso}H°$, and entropy, $\Delta_{iso}S°$—for the *trans* to *gauche* conformational isomerism of $[C_4mim]^+$ in liquid [C_4mim]X (X = Cl^-, Br^-, and I^-). The structures of [C_4mim]Cl (at various temperatures below and above its melting point) and of [C_4mim]Br (supercooled at ambient temperature) were also determined by means of HEXRD and MD simulations. Supplementary MD simulations were able to reproduce qualitatively the thermodynamic quantities and the liquid structures. The influence of the halide anion on the conformational isomerism of $[C_4mim]^+$ was discussed in terms of the corresponding liquid structures and of the cation−anion interactions present. Subsequent ab initio calculations for the [C_4mim]I ion pair in the gas phase also corroborated the experimental fact that the *gauche* isomers are stabilized by smaller halide anions *via* larger electrostatic contributions to the interactions between the ion pairs at contact.

Experiments and Theoretical Calculations

Materials. The [C_4mim]X (X = Cl^-, Br^-, and I^-) ionic liquid samples were synthesized by the usual route.[95–97] Water content was checked by Karl Fischer titration and found to be less than 20 ppm. All materials were treated and stored in a high performance glovebox (MIWA MFG Co. Ltd.), in which water and oxygen contents were kept at levels less than 1 ppm.

Raman Spectra Measurements and Data Analyses. The experimental methodology used during the Raman spectra measurements is similar to those of our previous Raman studies.[94,98–107] Temperature-dependent Raman measurements were carried out in the 298−400 K temperature range using a hermetically sealed quartz cell whose temperature fluctuations during the measurement were kept within ±0.3 K of the selected target temperature. The headspace in the sample cell was filled with dry nitrogen gas.

Throughout the paper, the equilibrium constant, K_{iso}, for the conformational isomerism between isomers A and B is defined as $K_{iso} = c_B/c_A$, with c_A and c_B denoting the concentration of each isomer. This means that $\Delta_{iso}G°$ is written as $\Delta_{iso}G° = -RT \ln K_{iso} = -RT \ln(c_B/c_A)$, where, *R* and *T* stand for the gas constant and temperature, respectively. If we take into consideration that the Raman band intensity, $I = Jc$, can be represented as the product between the Raman scattering coefficient, *J*, and the concentration of the scattering species, *c*, eq 1 can be derived.

$$-R \ln(I_B/I_A) = \Delta_{iso}H°/T - \Delta_{iso}S° - R(J_B/J_A) \quad (1)$$

where I_A and I_B and J_A and J_B denote the Raman band intensity and Raman scattering coefficients for the A and B isomers, respectively. I_A and I_B were estimated by nonlinear least-squares analyses using *pseudo*-Voigt functions represented as a linear combination of Gauss and Lorentz functions. Plots of $-R \ln(I_B/I_A)$ against reciprocal *T* yield $\Delta_{iso}H°$ as their slope. $\Delta_{sio}S°$ is also given from their intercept, if the corresponding ratio of Raman scattering coefficients (J_B/J_A) is known. Finally, $\Delta_{iso}G°$ can be evaluated from the simple relationship $\Delta_{iso}G° = \Delta_{iso}H° - T\Delta_{sio}S°$.

High-Energy X-ray Diffraction and Data Analysis. HEXRD measurements were carried out using the BL04B2 beamline of SPring-8 at the Japan Synchrotron Radiation Research Institute (JASRI).[108,109] The ionic liquid samples were set in a hermetically sealed capillary Pyrex glass tube of 3.5 mm diameter and 0.1 mm thickness. Monochromatic 61.6 keV X-rays were obtained using a Si(220) monochromator. The observed X-ray intensity was corrected for absorption[110] and polarization. Incoherent scatterings[111–113] were subtracted to obtain coherent scatterings, $I_{coh}(Q)$. The X-ray structure factor $S^{HEXRD}(Q)$ and X-ray radial distribution function $G(r)$ per stoichiometric volume were, respectively, obtained according to

$$S^{HEXRD}(Q) = \frac{I_{coh}(Q) - \sum n_i f_i(Q)^2}{(\sum n_i f_i(Q))^2} + 1 \qquad (2)$$

$$G^{HEXRD}(r) - 1 = \frac{1}{2\pi^2 r\rho_0}\int_0^{Q_{max}} Q\{S(Q) - 1\}\sin(Qr) \times \exp(-BQ^2)\mathrm{d}Q \qquad (3)$$

where n_i and $f_i(Q)$ denote the number and the atomic scattering factor of atom i,[114] respectively, ρ_0 is the number density, and B is the damping factor. All data treatment was carried out using the program KURVLR.[115]

MD Simulations. Although some new specific force fields have been developed recently,[116–122] we have decided to use the more general and transferable CLaP[123–126] force field in order to maintain consistency when comparing different halide-based ionic liquids. Therefore, the Lennard-Jones (LJ) parameters for the iodide anion were obtained from the Tosi and Fumi potentials,[127] with fitted parameters of $\varepsilon = 21.2$ kJ mol^{-1} and $\sigma = 4.42$ Å, validated by the experimental density of $[C_4mim]I$. All MD simulations in this study use force fields of the OPLS-AA kind.[128,129] In our simulations, Gear's predictor-corrector algorithm[130,131] was employed for integration of the equations of motion with 0.2 fs time steps. The systems contained 256 ion pairs under *NTP* ensemble conditions controlled by Nose's thermostat[132,133] and Parrinello−Rahman's barostat.[134,135] The latter was always set to atmospheric pressure. Long-range interactions were estimated using the Ewald summation method with real-space cutoff distances of 11 Å. The initial configurations were built using methodologies similar to those previously reported.[89–94,99] The simulation runs typically consisted of 2.5−3.5 ns equilibration periods followed by 0.5 ns production cycles, whose trajectories were then analyzed. All simulations were carried out using Fujitsu Materials Explorer 4.0 on the Fujitsu PRIMEQUEST 580 at the Computing and Communications Center, Kyushu University.

Experimental density values at 298 K for the three studied ionic liquids range from 1.08 to 1.10 g cm^{-3} for $[C_4mim]Cl$,[136,137] 1.30 g cm^{-3} for $[C_4mim]Br$,[138] and 1.44 to 1.46 g cm^{-3} for $[C_4mim]I$.[137,138] Simulated density values for these ionic liquids linearly decreased with increasing temperature; thus, values of slope and intercept of −0.00073 and 1.27, −0.00084 and 1.50, and −0.00034 and 1.56 were obtained for Cl-, Br-, and I-based ionic liquids, respectively. Extrapolated values at 298 K are 1.06(1), 1.25(2), and 1.46(1) for the respective ionic liquid, which means that the simulations can reproduce the experimental density with deviations of a few percentage points.

The X-ray structure factor $S^{MD}(Q)$ was calculated as

$$\begin{cases} S^{MD}(Q) = \dfrac{\sum_i \sum_j \{n_i(n_j - 1)\, f_i(Q)\, f_j(Q)/N(N-1)\}}{\{\sum_k (n_k f_k(Q)/N)\}^2} \times \\ \qquad \int_0^r 4\pi r^2 \rho_0 (g_{ij}^{MD}(r) - 1)\dfrac{\sin(Qr)}{Qr}\,\mathrm{d}r + 1 \qquad (i = j) \\ S^{MD}(Q) = \dfrac{\sum_i \sum_j (2 n_i n_j f_i(Q)\, f_j(Q)/N^2)}{\{\sum_k (n_k f_k(Q)/N)\}^2} \times \\ \qquad \int_0^r 4\pi r^2 \rho_0 (g_{ij}^{MD}(r) - 1)\dfrac{\sin(Qr)}{Qr}\,\mathrm{d}r + 1 \qquad (i \neq j) \end{cases} \qquad (4)$$

where ρ_0 denotes the ensemble average of the number density, and the total number of atoms in the simulation box N is given by

$$N = \sum_k n_k \qquad (5)$$

The X-ray radial distribution function $G^{MD}(r)$ was obtained from $S^{MD}(Q)$ by a Fourier transform procedure similar to that of $S^{HEXRD}(Q)$.

Molecular Orbital Calculations. The Gaussian 03 program[139] was used for DFT, MP2, and CCSD(T) calculations with basis sets implemented in the same program. DGDZVP basis sets[140] were used for iodide. Theoretical Raman bands were calculated at the B3LYP/6-311+G(d,p) level. The CCSD(T)/cc-pVTZ level calculations yielded the formation energies (E_{form}) of the conformational isomers of the $[C_4mim]I$ complex relative to its isolated ions. The estimation method was similar to the one previously used in the calculation of the conformational energies of the $[C_4mim]Cl$ and $[C_4mim]Br$ complexes.[72]

Results and Discussion

Dependence of $[C_4mim]^+$ Conformational Isomerism on the Size of the Halide Anion. Raman spectra of the $[C_4mim]X$ (X = Cl, Br, and I) ionic liquids at 348 K were recorded in the 550−790 cm^{-1} frequency range and are shown in Figure 1. The spectra are similar to those reported by Katayanagi et al.[24] and exhibit bands at 600, 624, 656, 667, 698, 726, and 755 cm^{-1}. According to Holomb et al., the two bands at 600 and 624 cm^{-1} can be ascribed to the *gauche* and *trans* isomers with respect to the N1−C7−C8−C9 dihedral angle such as ***GT*** (or ***GG***) and ***TG*** (or ***TT***), respectively. They found that the additional isomers *GG* and *TG* exist in $[C_4mim][BF_4]$ as minor species.[29] However, if one looks more carefully, the two dihedral angles under scrutiny may yield nine different conformers: for instance, the *GT* isomer can be subdivided into *GT* and *G′T* with N7−C7−C8−C9 dihedral angles of 60 and −60°, respectively. In other words, each gauche conformation has its mirror image.[30,77] When this analysis is applied to the two dihedral angles N1−C7−C8−C9 and C7−C8−C9−C10, nine possible conformers are generated. Theoretical Raman bands at the B3LYP/6-311+G(d,p) level for the nine isomers were calculated and are also shown in Figure 1. It is clear that Raman bands around 625 cm^{-1} (and also at 667 and 726 cm^{-1}) correspond to *trans* isomers relative to the N1−C7−C8−C9 angle such as ***TT***, ***TG***, and ***TG′***, whereas those around and below 600 cm^{-1} (and also at 698 cm^{-1}) correspond

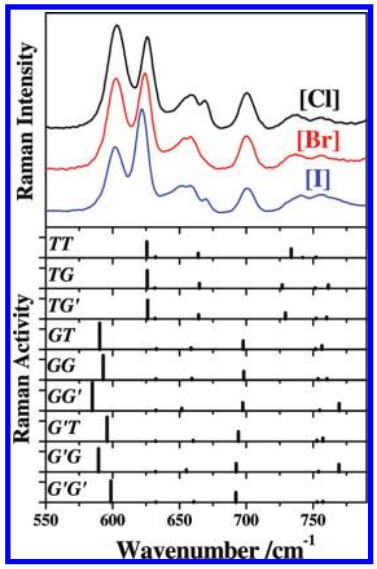

Figure 1. Raman spectra of [C_4mim][X] (X: Cl, Br, and I) ionic liquids at the frequency range 550−790 cm^{-1} recorded at 348 K. Upper, middle, and lower spectra were those for chloride, bromide, and iodide ionic liquids, respectively. Theoretical Raman bands for nine isomers with respect to the N1−C7−C8−C9 dihedral angle of the C_4mim^+ predicted at the B3LYP/6-311+G(d,p) level were also shown.

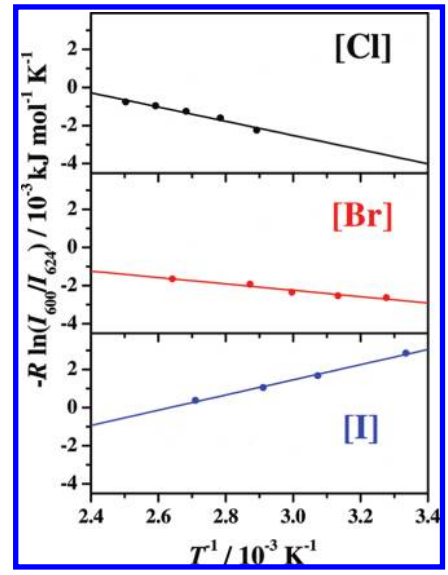

Figure 2. van't Hoff plots of the conformational isomerism of [C_4mim] from *trans* to *cis* isomers in chloride (upper), bromide (middle), and iodide (lower) ionic liquids, respectively, by Raman spectroscopy.

to *gauche* isomers relative to that same torsion angle, such as ***GG***, ***G′G′***, ***G′G***, ***GG′***, ***GT***, and ***G′T***. The frequencies of this latter set of isomers also depend significantly on the C7−C8−C9−C10 dihedral angle. Hereafter, unless stated otherwise, *trans* and *gauche* will designate the conformations relative to the N1−C7−C8−C9 dihedral angles. Figure 1 also shows that, as the halide ionic radius decreases, the intensity of the Raman bands at 600 cm^{-1} increases, while that of the bands at 624 cm^{-1} decreases. This indicates that *gauche* isomers prefer a stronger, more localized, negative electrostatic field formed by smaller anions surrounding the $[C_4mim]^+$ cation.

The relative intensities and areas of the bands at 600 and 625 cm^{-1} should reflect the relative amounts of the corresponding isomers, and thus allow calculation of the Gibbs free energy of the isomerization process. Moreover, the temperature dependence of the Raman spectra can yield thermodynamic quantities such as $\Delta_{iso}H°$ and $\Delta_{iso}S°$. An example of such dependence is shown in Figure S1 (in the Supporting Information) for the [C_4mim]Cl ionic liquid. The Raman bands were analyzed by nonlinear curve fitting with pseudo-Voigt peak functions to estimate the corresponding integral intensity and intensity ratios of the peaks (Figure S2, Supporting Information). As mentioned in the experimental section, the thermodynamic quantities for the isomerization equilibrium from A to B can be evaluated with van't Hoff-type plots of $-RT\ln(I_B/I_A)$ versus $1/T$. The plots for [C_4mim]Cl, [C_4mim]Br, and [C_4mim]I ionic liquids are shown in Figure 2, where the Raman bands at 600 and 624 cm^{-1} were analyzed as proxies for the *gauche* and *trans* isomers, respectively; i.e., $-RT\ln(I_{600}/I_{624})$ was plotted against $1/T$ to yield thermodynamic quantities related to the *trans*−*gauche* isomerization. As shown in Figure 2, all plots fall on the respective linear least lines within the errors. The corresponding slopes, that yield the values of $\Delta_{iso}H°$, show an obvious dependence with the nature of the anion, with positive values for [C_4mim]I and negative ones for [C_4mim]Cl and [C_4mim]Br.

Furthermore, if the Raman scattering coefficient ratio between the selected peaks, J_{600}/J_{624}, is known, then the value of $\Delta_{iso}S°$ can be assessed from the intercept of the plots. Here, the theoretical value for the J_{600}/J_{624} was estimated on the basis of ab initio calculations at the B3LYP/6-311+G(d,p) level. Finally, $\Delta_{iso}G°$ can be evaluated according to the definition of $\Delta_{iso}G° = \Delta_{iso}H° - T\Delta_{iso}S°$. The obtained values of $\Delta_{iso}G°$, $\Delta_{iso}H°$, and $\Delta_{iso}S°$ at 298 K are listed in Table 1, and plotted against Shannon's ionic radii of the halides[141] in Figure 3.

TABLE 1: Gibbs Free Energy $\Delta_{iso}G°$, Enthalpy $\Delta_{iso}H°$, and Temperature Multiplied Entropy $T\Delta_{iso}S°$ for the *TT* to *GT* (or *G′T*) Isomerization Process at 298 K

	[C_4mim][Cl]		[C_4mim][Br]		[C_4mim][I]	
	Raman	MD	Raman	MD	Raman	MD
$\Delta_{iso}G°$/kJ mol^{-1}	0.0(5)	−3.1(3)	0.3(2)	−2.3(3)	2.0(2)	2.4(1)
$\Delta_{iso}H°$/kJ mol^{-1}	−3.7(4)	−2.8(2)	−1.6(2)	−2.3(3))	3.9(2)	0.4(1)
$T\Delta_{iso}S°$/kJ mol^{-1}	−3.6(3)	0.2(2)	−2.0(2)	0.1(1)	1.9(2)	0.0(0)

As it can be seen in Figure 3, the values of $\Delta_{iso}G°$ are close to zero, which indicates that the *trans* and *gauche* isomers coexist in comparable quantities in the studied ionic liquids. However, a small but significant trend is observed: $\Delta_{iso}G°$ becomes more negative with the decrease of the halide ionic

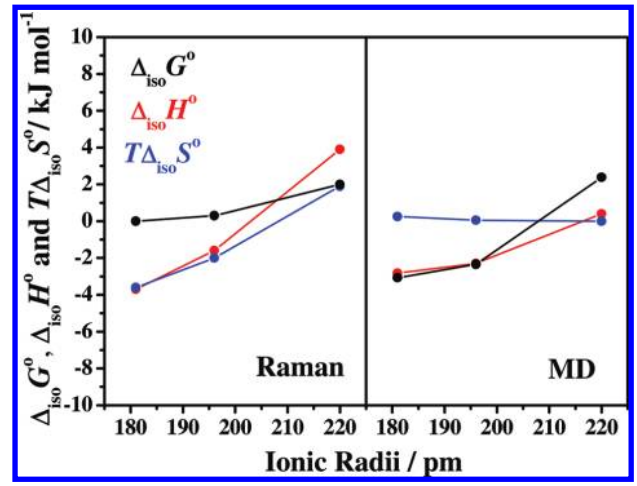

Figure 3. Thermodynamic quantities for the conformational isomerism of [C_4mim] from *trans* to *cis* isomers as a function of anion ionic radii evaluated by Raman spectroscopy (left) and MD simulations (right), respectively.

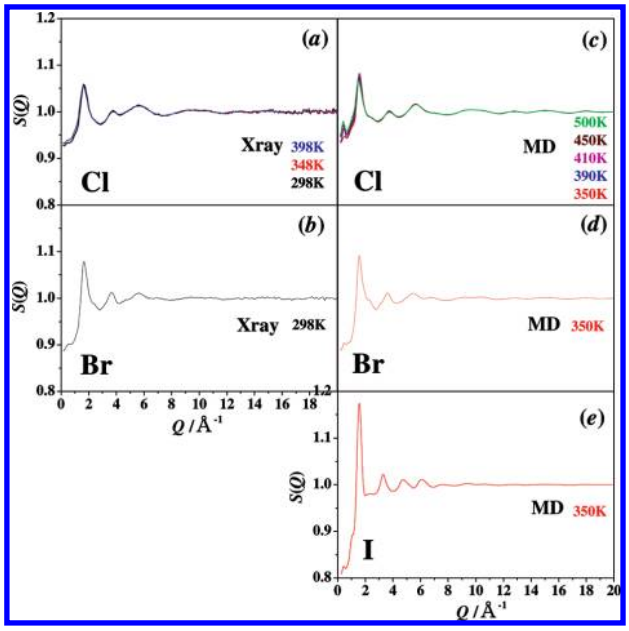

Figure 4. X-ray structure factors (a) for [C4mim][Cl] measured at 298, 348, and 398 K and (b) that for [C4mim][Br] at 298 K. Those derived from MD simulations were also shown in panels c, d, and e for [C4mim][Cl] at various temperatures, [C4mim][Br] at 350 K, and [C4mim][I] at 350 K, respectively.

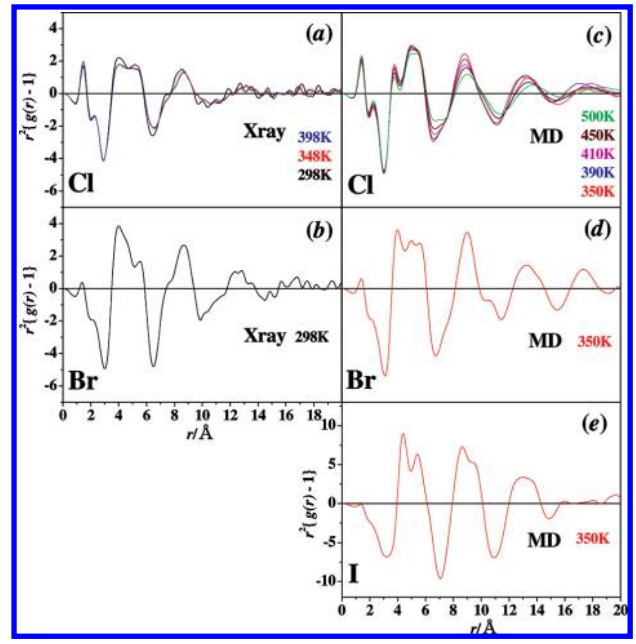

Figure 5. Difference radial distribution functions as the form of $r^2\{G(r) - 1\}$ (a) for [C4mim][Cl] measured at 298, 348, and 398 K and (b) that for [C4mim][Br] at 298 K. Those derived from MD simulations were also shown in panels c, d, and e for [C4mim][Cl] at various temperatures, [C4mim][Br] at 350 K, and [C4mim][I] at 350 K, respectively.

radius. Clearly, the *gauche* isomers are stabilized relative to their *trans* counterparts when the $[C_4mim]^+$ cation experiences a more negative electrostatic field from the surrounding halide ions. Such a trend is even more noticeable in $\Delta_{iso}H°$. In other words, the relative stabilization of *gauche* isomers is enthalpically driven by the surrounding halide ions. In addition, it is worth mentioning that $T\Delta_{iso}S°$ also becomes more negative with the decrease of the halide radius, thus compensating the $\Delta_{iso}H°$ trend and leading to rather small $\Delta_{iso}G°$ values. This compensation between $\Delta_{iso}H°$ and $T\Delta_{iso}S°$ is also shown in Figure S3 (Supporting Information), where $T\Delta_{iso}S°$ was plotted against $\Delta_{iso}H°$. Such strong compensation (and correlation) implies that the stronger interactions between the smaller halide ions and the $[C_4mim]^+$ cation (enthalpic merit) are linked to more limited orientations or configurations between the ions (entropic demerit).

Liquid Structure of [C4mim]X (X = Cl−, Br−, and I−) Ionic Liquids. Experimental X-ray structure factors for [C4mim]Cl at 298, 348, and 398 K and for [C4mim]Br at 298 K are shown in Figure 4. The high-Q regions above 3 $Å^{-1}$ exhibit oscillations that are common to all ionic liquids, suggesting that the X-ray structure factor in this region is able to reflect adequately the intramolecular structure of the $[C_4mim]^+$ cation in the ionic liquids. On the other hand, the low-Q regions below 3 $Å^{-1}$ exhibit an intense peak at 1.63 $Å^{-1}$ with a shoulder around 2.5 $Å^{-1}$ for [C4mim]Cl and a main peak at 1.67 $Å^{-1}$ with a shoulder at 2.4 $Å^{-1}$ for [C4mim]Br, respectively. This indicates that these ionic liquids have considerable long-range ordering. Moreover, the positions and intensities of the X-ray structure-factor spectra of [C4mim][Cl] are temperature-independent in the studied temperature range, which strongly suggests that there are no significant changes in the liquid structure of [C4mim]Cl as the temperature is raised from room temperature to a value 100 °C above it. It also suggests that the cation−anion potential well in [C4mim]Cl is rather deep and narrow, which may be a specific feature of these ionic liquids, especially if one compares it with the situation in water or in other nonaqueous molecular solvents. Finally, the positions of the main peak and its shoulder are almost the same for [C4mim]Cl and [C4mim]Br, which indicates that long-range ordering is similar for both ionic liquids.

It is possible to compare the X-ray structure factors obtained with those available for other ionic liquids. The most important issue to point out is that the main low-Q peak that was observed for [C4mim]Cl and [C4mim]Br also shows up as a single peak in [C4mim]I,[24] [C4mim][PF_6],[81] fluorohydrogenated ionic liquids such as [C_1im]F·2.3HF (C_1im = 1-methylimidazolium) and [$C_n$mim]F·2.3HF (n = 2, 4, and 6),[87] [C2mim][BF_4][90] and [C4mim][BF_4],[78] and [C2mim][FSA] (FSA = bis(fluoromethanesulfonyl)amide).[94] On the other hand, TFSA-based ionic liquids combined with $[C_2mim]^+$,[93] $[C_4mim]^+$, $[C_4dmim]^+$ (C_4dmim = 1-butyl-2,3-dimehtylimidazolium),[89] and $[C_4mpyrr]^+$ (C_4mpyrr = *N*-butyl-*N*-methylpyrrolidinium)[93] exhibit low-Q structure factors with two distinct main peaks. Finally, X-ray structure factors for [C_2am][NO_3] (C_2am = ethylammonium)[92] and [$P_{6\,6\,6\,14}$]Cl ($P_{6\,6\,6\,14}$: trihexyltetradecylphosphonium)[79] ionic liquids found in very recent publications show only an intense single peak in the low-Q region. Therefore, the splitting into two distinct peaks is specific to TFSA-based ionic liquids.

Figure 5 shows difference radial distribution functions in the form of $r^2\{G(r) - 1\}$ for [C4mim]Cl and [C4mim]Br at the corresponding measured temperatures. Sharp peaks at 1.45 and 2.35 Å are ascribable to intramolecular atom−atom correlations in the $[C_4mim]^+$ cation of both bonding and nonbonding nature. Concerning the intermolecular correlations, broad peaks centered at around 5, 8, and 13 Å were obtained for both ionic liquids. These peak positions are similar to those observed for [C4mim]I and reported by Katayanagi et al.[24] Although the ionic radii of Cl^- (1.81 Å), Br^- (1.96 Å), and I^- (2.20 Å) are rather different, it is interesting to notice that the broad peaks originating from the intermolecular correlations appear centered at similar positions. This indicates that, for all studied ionic liquids, the spatial distribution of the halide ions around the $[C_4mim]^+$ cation

is, in broad terms, not very different. This supports the previous discussion based on the strong compensation between $\Delta_{iso}H°$ and $\Delta_{iso}S°$.

On the other hand, the shape of those broad peaks is slightly different in each case; for instance, the broad peaks around 5 Å consist of subpeaks at 4.0 and 5.2 Å for [C_4mim]Cl and subpeaks at 4.0, 4.6 (shoulder), and 5.5 Å for [C_4mim]Br. The corresponding subpeaks for [C_4mim]I are localized at 4.5 and 5.5 Å.[24] The broad peak centered at around 5 Å can be mainly ascribed to the first shell cation−anion correlations in the ionic liquid, which are composed by the closest neighbor atom−atom pair correlations, and the subsequent second- and third-neighbor ones. It is supposed that the closest neighbor atom−atom correlation distance should increase with the increase of the halide ionic radius. However, the peaks at 4.0 Å that were observed for both the chloride and bromide ionic liquids are practically independent from the halide radii, suggesting that these peaks reflect second-neighbor atom−atom correlations or that in this case the contribution from the closest neighbor atom−atom correlation is not so important because there is no preferred closest neighbor ion pair. In general, second-neighbor correlations also depend on the orientation among interacting pairs, which means that similar correlation distances can occur even when the size of one of the species is increased. On the other hand, the variation of the shape of the broad peak around 5 Å implies that the mutual orientations and configurations of the second-shell ion pairs are more dependent on the nature of the halide.

Ion−Ion Interactions in the Ionic Liquids. Several MD simulations dealing with [C_4mim]X (X = Cl^-, Br^-, and I^-) ionic liquids have been reported. Urahata and Ribeiro inferred the liquid structure and dynamics of [$C_n$mim]Cl and [C_4mim]Br using united-atom simulations.[142–144] Raabea and Köhler have also explored the thermodynamic and structural properties of [$C_n$mim]Cl using united-atom models.[145,146] Alavi investigated the dynamics and transport properties of similar systems.[147,148] SO_2−[C_4mim]Br systems have been reported by Ando and Santos.[149] Schröder et al. studied [C_4mim]I using 100 ns long simulations.[150] Car−Parinnello molecular dynamics simulations have also been carried out by Ghatee and Ansari.[151] Qiao et al. reported structural and dynamic aspects of [C_2mim]Cl in terms of anion effects.[152] In addition, Remsin et al. investigated [C_4mim]Cl in water and in dimethylsulfoxide solutions.[153] The conformational isomerism of the [C_4mim]$^+$ cation and the corresponding X-ray/neutron weighted structure factors for [C_4mim]X were almost not discussed in these studies. Therefore, we felt that a more detailed analysis of the ion−ion interactions in the studied ionic liquids using MD simulation, and taking into account the two points just mentioned, was necessary at this stage.

First, dihedral angle distributions with respect to the N1−C7−C8−C9 angle in the [C_4mim]$^+$ cation were analyzed. Results for [C_4mim]Cl are shown in Figure S4 of the Supporting Information (these are also representative of the other ionic liquids). At all temperatures examined, the figure clearly shows two peaks at 60 and 300° corresponding to the *gauche* (*G*, *G′*) isomers and one peak at 180° corresponding to the *trans* (*T*) isomer. At the lowest temperature (350 K), the *gauche* isomer peaks are larger than that of the *trans* isomer, indicating that *gauche* isomers are more abundant than *trans* ones. With increasing temperature, the combined height of the *gauche* isomer peaks decreases more rapidly than that of the *trans* isomer, suggesting that the *gauche* isomer is enthalpically more stable than the *trans* one. At the highest temperature (500 K), the *gauche/trans* relative peak height is reversed when comparing it with the values at the lowest temperature. Thus, MD simulations are able to reproduce the experimental Raman spectroscopy results. The amount of each isomer was calculated *via* integration of the corresponding distribution histograms (the integrated intensities were evaluated by nonlinear curve fitting using Gaussian functions) in order to estimate thermodynamic quantities such as $\Delta_{iso}G°$, $\Delta_{iso}H°$, and $\Delta_{iso}S°$. The van't Hoff-type plots are shown in Figure S5 (Supporting Information), in which experimental data are also shown for comparison. It is obvious that the isomerization thermodynamic quantities were successfully captured by the MD simulations, although the data for [C_4mim]I are relatively scattered. The obtained thermodynamic quantities are also shown in Figure 3. The MD simulations can reproduce the experimental trends; i.e., $\Delta_{iso}G°$ and $\Delta_{iso}H°$ become more negative as the halide ionic radii are decreased.

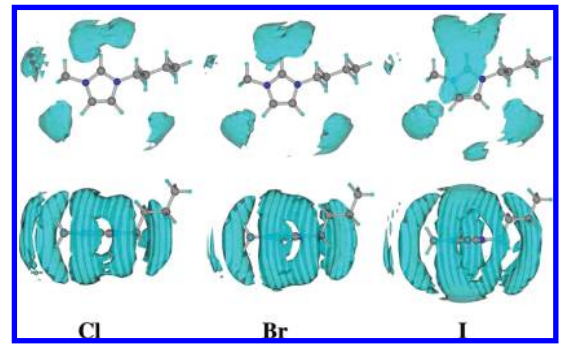

Figure 6. Spatial distribution functions of halide anions around the C2 carbon in the imidazolium ring for [C_4mim][X] (X: Cl^-, Br^-, and I^-) ionic liquids.

Liquid structures of [C_4mim]X (X = Cl^-, Br^-, and I^-) were also explored by MD simulation. Structure factors for [C_4mim]Cl and [C_4mim]Br derived from the MD trajectories are shown in Figure 4. The peak and trough positions of the experimental X-ray structure factors are correctly reproduced by the MD simulations, although the corresponding oscillation amplitudes are slightly overestimated. Radial distribution functions obtained by MD are also shown in Figure 5. The long-range ordering represented by the peak and trough positions of the broad peaks arising from the interionic correlations is well produced by the simulations. On the other hand, the oscillation amplitudes and the peak shape are slightly different from the experimental results. Thus, we can state that the simulations can qualitatively reproduce the liquid structure and ion−ion interactions in these ionic liquids.

Though qualitative, the MD simulations can provide other valuable structural information such as the spatial distribution functions (SDFs) of the halide ions around the [C_4mim]$^+$ cation in the studied ionic liquids. SDFs for [C_4mim]X (X = Cl^-, Br^-, and I^-) are shown in Figure 6. SDFs for [C_4mim]Cl[139,142] and [C_4mim]I[147] have already been reported, and those calculated in this study are in good agreement with the previous ones. As shown in Figure 6, the SDFs are similar for the three studied ionic liquids: in all cases, the halide ions cluster around the positively charged hydrogen atoms of the imidazolium ring such as C_2−H, C_4−H, and C_5−H. However, some differences are noticeable for the iodide-based ionic liquid. In this case, the halide population facing the C_2−H atom decreases and is compensated by an increase in the population above and below the imidazolium ring plane. This implies that larger halide ions contribute less in terms of electrostatic or specific interactions to the overall interaction between close-contact ion pairs.

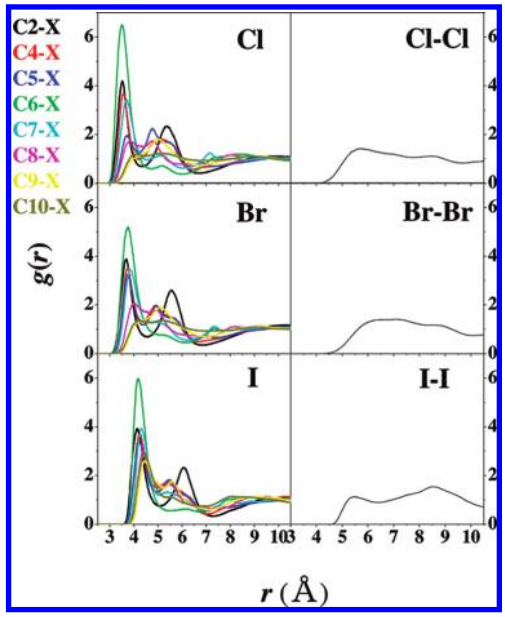

Figure 7. Partial pair correlation functions between carbon atoms in [C4mim] and halide anions (left panels) and those among halide anions (right) for Cl^- (top), Br^- (middle), and I^- (bottom) ionic liquid, respectively.

Clearly, the SDFs support the Raman experimental findings that suggest *gauche* isomers to be the preferred species in stronger and more localized electrostatic fields. In addition, SDFs also illustrate the correct structural information (and agree with HEXRD experiments), showing that the mutual orientation and configuration between the cation and anion are strongly dependent on the size of the halide ion.

Partial pair correlation functions, $g_{Cn-X}(r)$, between a given carbon atom (C*n*) of the cation and anion X^- are shown in Figure 7 for the ionic liquids [C4mim]X (X = Cl^-, Br^-, and I^-) at 350 K. As expected, the position of the first peak of each $g_{Cn-X}(r)$ function is shifted to longer distances as the anion size is increased. On the other hand, in terms of the carbon atom under scrutiny, the order of intensity of the first peaks is, for all studied ionic liquids, C6 > C2 > C4, C5, C7 > C8, C9, C10. Such order is a clear indication of the prevalent interactions between the ions and also of the existence of polar and nonpolar domains in the ionic liquid:[52] C2 ≤ C*n* ≤ C7 belong to the polar domain, whereas C8 ≤ C*n* ≤ C10 are part of the nonpolar domain; the higher intensity of the C6 carbon is just an indication of its lack of stereochemical constraints (a terminal methyl carbon); the larger intensity of C2 relative to C4 or C5 denotes the higher acidity of the hydrogen atom bonded to the first and its ability to establish stronger interactions with the anions.

It must be pointed out that in [C4mim]I the C8−I, C9−I, and C10−I rdf's (carbon atoms from the nonpolar domain) show first peaks that are comparable in intensity to those of the carbon atoms belonging to the polar domain. This clearly indicates the subdued electrostatic nature of the interactions with the iodide anion and the relative importance of van der Waals interactions in this case.

Finally, we have also analyzed the anion−anion correlation functions in the three studied ionic liquids. The corresponding rdf's are shown in Figure 7. Clearly, the rdf's for the Cl^- and Br^- ionic liquids are similar to each other, while that for the I^- ionic liquid has a rather different trend. The crystalline structures of the three compounds[21,23,154] show anion−anion configurations that are considerably different from those in the liquid. However, some comparisons are possible: in both [C4mim]Cl and [C4mim]Br crystals, the Cl^- and Br^- anions are integrated in zigzag structures with characteristic distances of 4.65, 6.45, and 8.05 Å and 4.77, 6.55, and 8.30 Å, respectively.[24] In the [C4mim]I crystal, a less ordered array of anions with a broader distribution of characteristic distances (6.03, 7.06, 7.25, 7.74, 7.86, 8.28, and 9.01 Å) is found.[154] Although the order of the first peaks in the crystal and in the liquid phase is not maintained, one can argue that the broader distribution of the iodide anion in the crystal (where due to its less electrostic, more polarizable nature it is not so rigidly constrained into zigzag structures) is somewhat transferred to the liquid (where it can even permeate part of the nonpolar domains).

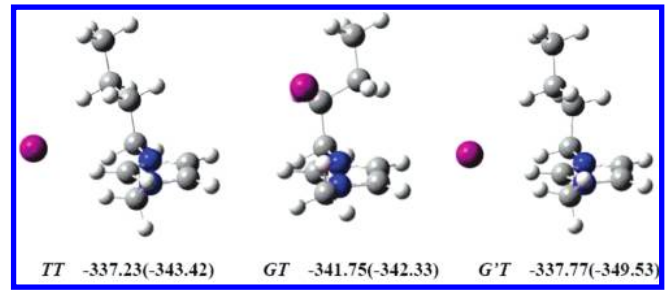

Figure 8. Optimized geometries at the MP2/6-311G(d,p) estimated formation E_{form} energies at the CCSD(T)/cc-pVTZ level for three isomers of the [C4mim][I] complexes. The E_{form} was given as the sum of the interaction energy (E_{int}) and the deformation energy (E_{def}) ($E_{form} = E_{int} + E_{def}$), and E_{int} is shown in parentheses. The I^- ion is in close contact with the C_2−H of the imidazolium in the *TT* and *G′T* isomers, while it is above the imidazolium ring in the *GT* isomer.

Geometries and Relative Energies for Isomers of [C4mim]I. The geometries of the three isomers of the [C4mim]I ion pair, optimized ab initio at the MP2/6-311G(d,p) level, and the corresponding energies of formation relative to the isolated ions, E_{form}, estimated at the CCSD(T)/cc-pVTZ level are shown in Figure 8. The iodide anion is in close contact with the C_2−H hydrogen atom of the imidazolium ring in both optimized geometries for the *TT* and *G′T* isomers, while it is above the imidazolium ring in the *GT* isomer. In the case of the [C4mim]Cl and [C4mim]Br ion pairs, it was found that all optimized geometries of the three isomers show the anions in close contact with the C_2−H hydrogen atom.[72] The calculations at the MP2/6-311G(d,p) level have also shown that the Cl^- and Br^- anions prefer interactions with the C_2−H in [C4mim]Cl and [C4mim]Br ion pairs but that in the [C4mim]I pair the two structures—iodide in contact with C_2−H versus iodide above the imidazolium plane—are nearly isoenergetic.[73] The intensity of the electrostatic interactions is responsible for these two different orientational preferences: the stabilization by the electrostatic interactions in the former structure is larger than that in the latter one in the [C4mim]Cl and [C4mim]Br complexes, whereas the electrostatic energies in the two structures are nearly identical in the [C4mim]I complex.[73] The SDFs obtained by the MD simulations (Figure 8) show that the anion population above and below the imidazolium plane in the [C4mim]I ionic liquid is larger than that in the [C4mim]Cl ionic liquid. The orientational preference in the two complexes obtained by the ab initio calculations explains very well the different behavior observed in the SDFs of the two ionic liquids.

The E_{form} calculated for the *GT* isomer relative to that for the *TT* isomer is −4.52 kJ/mol in the [C4mim]I complex. The E_{form} for the *G′T* isomer is close to that of the *TT* isomer. The energy of an isolated *GT* isomer relative to an isolated *TT* isomer

(no iodide, just the cation) calculated at the same level is −0.08 kJ/mol.[72] This shows that the interactions with the I^- increase the relative stability of the *GT* isomer substantially. The stabilization of the *GT* isomer was also observed in the $[C_4mim]Cl$ and $[C_4mim]Br$ complexes. The energies of the *GT* isomers of the $[C_4mim]Cl$ and $[C_4mim]Br$ complexes relative to the *TT* isomers calculated at the same level are −5.36 and −4.77 kJ/mol, respectively.[72] The order of the magnitude of the stabilization of the *GT* isomer is $Cl^- > Br^- > I^-$, which coincides with the observed order of $\Delta_{iso}H°$.

The charge distributions of the *TT* and *GT* isomers of the $[C_4mim]^+$ cation suggest that the electrostatic interactions with the anion are responsible for the stabilization of the *GT* isomer. The atomic charge distributions for the *TT* and *GT* isomers of an isolated $[C_4mim]^+$ calculated from the MP2/6-311G(d,p) level wave functions show that the C_2-H group in the *GT* isomer has a substantial positive charge (+0.08*e*), while the positive charge is smaller in the *TT* isomer (+0.03*e*).[72] This shows that the stabilization of the *GT* isomer by the electrostatic interactions is larger than that of the *TT* isomer. The magnitude of the electrostatic interactions increases with a decrease in the anion size, which explains the trend of $\Delta_{iso}H°$. The electrostatic interactions calculated for the most stable orientations of the $[C_4mim]Cl$, $[C_4mim]Br$, and $[C_4mim]I$ complexes (*GT* isomers) are −364.2, −346.5, and −320.3 kJ/mol, respectively.[73]

Conclusion

The thermodynamic quantities $\Delta_{iso}G°$, $\Delta_{iso}H°$, and $\Delta_{sio}S°$ at 298 K for the *trans* to *gauche* isomerization of the $[C_4mim]^+$ cation in $[C_4mim][X]$ ($X = Cl^-$, Br^-, and I^-) ionic liquids were evaluated using Raman spectra obtained at different temperatures. Values of $\Delta_{iso}G°$ for these ionic liquids are nearly close to zero, although small but significant shifts could be determined; i.e., $\Delta_{iso}G°$ values become more negative with decreasing halide ion size. This trend was also clearly observed in the variations of $\Delta_{iso}H°$ and $\Delta_{iso}S°$, suggesting that the *gauche* isomers of the $[C_4mim]^+$ cation are more stabilized in the more electronegative field caused by smaller halide ions. To obtain further insight into the $[C_4mim]^+-X^-$ interaction in the ionic liquids, X-ray structure factors and X-ray radial distribution functions for $[C_4mim]Cl$ and $[C_4mim]Br$ ionic liquids were evaluated by HEXRD experiments at temperatures around or above their melting points. Broad peaks of 5, 8, and 13 Å ascribable to the intraionic correlations were similar for both ionic liquids, and also resembled those observed for the $[C_4mim]I$ ionic liquid. On the other hand, the shape of the broad peaks centered at around 5 Å arising from the closest cation−anion interactions was noticeably different among them, indicating that the relative orientation and/or configuration between cation and anion significantly varied with the size of the anion.

The conformational isomerism of the $[C_4mim]^+$ cation, the liquid structure, and the ion−ion interactions in these ionic liquids were also analyzed with the aid of MD simulations. MD simulations qualitatively reproduced the isomerization thermodynamic quantities obtained *via* Raman spectroscopy and structure factors obtained by X-ray diffraction. SDFs of the anions around the imidazolium C_2-H hydrogen atom for all the studied ionic liquids exhibit similar features; i.e., the halide anions cluster around the positively charged hydrogen atoms of the imidazolium such as C_2-H, C_4-H, and C_5-H. However, in the $[C_4mim]I$ ionic liquid, the anion population facing the C_2-H decreases and is compensated by a population increase above and below the imidazolium ring plane. This corroborates the fact that larger anions contribute less to the electrostatic interactions between the contact ion pairs. Optimized geometries obtained ab initio at the MP2/6-311G(d,p) level for the isolated $[C_4mim]I$ complex and energies of formation for all of the $[C_4mim]X$ complexes obtained at the CCSD(T)/cc-pVTZ level support the above-mentioned experimental and MD simulation results. The present set of extensive and self-consistent data allowed us to conclude that the *gauche* isomers of the $[C_4mim]^+$ ion, particularly the *GT* conformation, are stabilized by the electrostatic interactions between the cation and the surrounding halide anions.

Acknowledgment. This work has been financially supported by Grant-in-Aids for Scientific Research No. 19003963, 19350033, and 20350037, and for Scientific Research in Priority Area (Ionic Liquids) 20031024 from the MEXT. HEXRD experiments were performed as the proposal No. 2007B1377 and 2009B1199 of SPring-8.

Supporting Information Available: Figures showing the temperature dependence of Raman spectra, typical extracted single Raman bands, $\Delta_{iso}H°$ and $T\Delta_{iso}S°$ correlation, the temperature dependence of the dihedral angle distribution, and van't Hoff plots. This material is available free of charge via the Internet at http://pubs.acs.org.

References and Notes

(1) *Ionic Liquids in Syntheses*, 2nd ed.; Wasserscheid, P., Welton, T., Eds.; VCH-Wiley: Weinheim, Germany, 2007; Vols. 1 and 2.
(2) *Ionic Liquids IV*; Brennecke, J. F., Rogers, R. D., Seddon, K. R., Eds.; ACS Symposium Series 975; Oxford University Press: 2007.
(3) *Electrochemical Aspects of Ionic Liquids*; Ohno, H., Ed.; Wiley-Interscience: Hoboken, NJ, 2005.
(4) Weingärtner, H. *Angew. Chem., Int. Ed.* **2008**, *47*, 654–970.
(5) Ludwig, R.; Krag, U. *Angew. Chem., Int. Ed.* **2007**, *46*, 6582–6584.
(6) Slattery, J. M.; Daguenet, C.; Dyson, P. J.; Schubert, T. J. S.; Krossing, I. *Angew. Chem., Int. Ed.* **2007**, *46*, 5384–5388.
(7) Wasserscheid, P.; Keim, W. *Angew. Chem., Int. Ed.* **2000**, *39*, 3772–3789.
(8) Endo, T.; Kato, T.; Tozaki, K.; Nishikawa, K. *J. Phys. Chem. B* **2010**, *114*, 407–411.
(9) Kawahata, M.; Endo, T.; Seki, H.; Nishikawa, K.; Yamaguchi, K. *Chem. Lett.* **2009**, *38*, 1136–1137.
(10) Nishikawa, K.; Wang, S.; Endo, T.; Tozaki, K. *Bull. Chem. Soc. Jpn.* **2009**, *82*, 806–812.
(11) Endo, T.; Nishikawa, K. *J. Phys. Chem. A* **2008**, *112*, 7543–7550.
(12) Nishikawa, K.; Wang, S.; Tozaki, K. *Chem. Phys. Lett.* **2008**, *458*, 88–91.
(13) Nishikawa, K.; Wang, S.; Katayanagi, H.; Hayashi, S.; Hamaguchi, H.; Koga, Y.; Tozaki, K. *J. Phys. Chem. B* **2007**, *111*, 4894–4900.
(14) Paulechka, Y. U.; Kabo, G. J.; Blokhin, A. V.; Shaplov, A. S.; Lozinskaya, E. I.; Golovanov, D. G.; Lyssenko, K. A.; Korlyukov, A. A.; Vygodskii, Y. S. *J. Phys. Chem. B* **2009**, *113*, 9538–9546.
(15) Blokhin, A. V.; Paulechka, Y. U.; Strechan, A. A.; Kabo, G. J. *J. Phys. Chem. B* **2008**, *112*, 4357–4364.
(16) Paulechka, Y. U.; Blokhin, A. V.; Kabo, G. J.; Strechan, A. A. *J. Chem. Thermodyn.* **2007**, *39*, 866–877.
(17) Blokhin, A. V.; Paulechka, Y. U.; Kabo, G. J. *J. Chem. Eng. Data* **2006**, *51*, 1377–1388.
(18) Berg, R. W. Raman spectroscopy, ab initio model calculations and conformational equilibria in ionic liquids. In *Ionic Liquids in Chemical Analysis*; Koel, M., Ed.; CRC Press: 2009.
(19) Berg, R. W. *Monatsh. Chem.* **2007**, *138*, 1045–1075.
(20) Hayashi, S.; Ozawa, R.; Hamaguchi, H. *Chem. Lett.* **2003**, *32*, 498–499.
(21) Saha, S.; Hayashi, S.; Kobayashi, A.; Hamaguchi, H. *Chem. Lett.* **2003**, *32*, 740–741.
(22) Ozawa, R.; Hayashi, S.; Saha, S.; Kobayashi, A.; Hamaguchi, H. *Chem. Lett.* **2003**, *32*, 948–949.
(23) Holbrey, J. D.; Reichert, W. M.; Nieuwenhuyzen, M.; Johnston, S.; Seddon, K. R.; Rogers, R. D. *Chem. Commun.* **2003**, 1636–1637.
(24) Katayanagi, H.; Hayashi, S.; Hamaguchi, H.; Nishikawa, K. *Chem. Phys. Lett.* **2004**, *392*, 460–464.

(25) Berg, R. W.; Deetlefs, M.; Seddon, K. R.; Shim, I.; Thompson, J. M. *J. Phys. Chem. B* **2005**, *109*, 19018–19025.
(26) Heimer, N. E.; Del Sesto, R. E.; Meng, Z.; Wilkes, J. S.; Carper, W. R. *J. Mol. Liq.* **2006**, *124*, 84–95.
(27) Katsyuba, S. A.; Zvereva, E. E.; Vidis, A.; Dyson, P. J. *J. Phys. Chem. A* **2007**, *111*, 352–370.
(28) Jeon, Y.; Sung, J.; Seo, C.; Lim, H.; Cheong, H.; Kang, M.; Moon, B.; Ouchi, Y.; Kim, D. *J. Phys. Chem. B* **2008**, *112*, 4735–4740.
(29) Holomb, R.; Martinelli, A.; Albinsson, I.; Lassègues, J. C.; Johansson, P.; Jacobsson, P. *J. Raman Spectrosc.* **2008**, *39*, 793–805.
(30) Paulechka, Y. U.; Kabo, G. J.; Emel'yanenko, V. N. *J. Phys. Chem. B* **2008**, *112*, 15708–15717.
(31) Chang, H.-C.; Jiang, J.-C.; Su, J.-C.; Chang, C.-Y.; Lin, S. H. *J. Phys. Chem. A* **2007**, *111*, 90201–9206.
(32) Chang, H.-C.; Chang, C.-Y.; Su, J.-C.; Chu, W.-C.; Jiang, J.-C.; Lin, S.-H. *Int. J. Mol. Sci.* **2006**, *7*, 417–424.
(33) Koeddermann, T.; Fumino, K.; Ludwig, R.; Canongia Lopes, J. N.; Pádua, A. A. H. *ChemPhysChem* **2009**, *10*, 1181–1186.
(34) Borodin, O. *J. Phys. Chem. B* **2009**, *113*, 12353–12357.
(35) Borodin, O. *J. Phys. Chem. B* **2009**, *113*, 11463–11478.
(36) Wang, Y. *J. Phys. Chem. B* **2009**, *113*, 11058–11060.
(37) Zhao, W.; Leroy, F.; Heggen, B.; Zahn, S.; Kirchner, B.; Balasubramanian, S.; Müller-Plathe, F. *J. Am. Chem. Soc.* **2009**, *131*, 15825–15833.
(38) Zhao, W.; Leroy, F.; Balasubramanian, S.; Müller-Plathe, *J. Phys. Chem. B* **2008**, *112*, 8129–8133.
(39) Sarangi, S. S.; Bhargava, B. L.; Balasubramanian, S. *Phys. Chem. Chem. Phys.* **2009**, *11*, 8745–8751.
(40) Bhargava, B. L.; Klein, M. L.; Balasubramanian, S. *ChemPhysChem* **2008**, *9*, 67–70.
(41) Bhargava, B. L.; Devane, R.; Klein, M. L.; Balasubramanian, S. *Soft Matter* **2007**, *3*, 1395–1400.
(42) De Andrade, J.; Böes, E. S.; Stassen, H. *J. Phys. Chem. B* **2008**, *112*, 8966–8974.
(43) Schröder, C.; Haberler, M.; Steinhausera, O. *J. Chem. Phys.* **2008**, *128*, 134501/1–134501/10.
(44) Schröder, C.; Rudas, T.; Neumayr, G.; Gansterer, W.; Steinhausera, O. *J. Chem. Phys.* **2007**, *127*, 044505/1−044505/10.
(45) Dávila, M. J.; Aparicio, S.; Alcalde, R.; García, B.; Leal, J. M. *Green Chem.* **2007**, *9*, 221–232.
(46) Eduardo, C.; Prado, R.; Carlos, L.; Freitas, G. *THEOCHEM* **2007**, *847*, 93–100.
(47) Picálek, J.; Kolafa, J. *J. Mol. Liq.* **2007**, *134*, 29–33.
(48) Bagno, A.; D'Amico, F.; Saielli, G. *J. Mol. Liq.* **2007**, *131*−*132*, 17–23.
(49) Bagno, A.; D'Amico, F.; Saielli, G. *J. Phys. Chem. B* **2006**, *110*, 23004–23006.
(50) Kelkar, M. S.; Maginn, E. J. *J. Phys. Chem. B* **2007**, *111*, 9424–9427.
(51) Santos, L. M. N. B. F.; Lopes, J. N. C.; Coutinho, J. A. P.; Esperancü, J. M. S. S.; Gomes, L. R.; Marrucho, I. M.; Rebelo, L. P. N. *J. Am. Chem. Soc.* **2007**, *129*, 284–285.
(52) Lopes, J. C. N.; Pádua, A. A. H. *J. Phys. Chem. B* **2006**, *110*, 3330–3335.
(53) Chaumont, A.; Wipff, G. *New J. Chem.* **2006**, *30*, 537–545.
(54) Buehl, M.; Chaumont, A.; Schurhammer, R.; Wipff, G. *J. Phys. Chem. B* **2005**, *109*, 18591–18599.
(55) Urukova, I.; Vorholz, J.; Maurer, G. *J. Phys. Chem. B* **2005**, *109*, 12154–12159.
(56) Del Popolo, M. G.; Lynden-Bell, R. M.; Kohanoff, J. *J. Phys. Chem. B* **2005**, *109*, 5895–5902.
(57) Del Popolo, M. G.; Voth, G. A. *J. Phys. Chem. B* **2004**, *108*, 1744–1752.
(58) Shim, Y.; Choi, M. Y.; Kim; Hyung, J. *J. Chem. Phys.* **2005**, *122*, 044511/1−044511/12.
(59) Shim, Y.; Choi, M. Y.; Kim; Hyung, J. *J. Chem. Phys.* **2005**, *122*, 044510/1−044510/12.
(60) Liu, Z.; Huang, S.; Wang, W. *J. Phys. Chem. B* **2004**, *108*, 12978–12989.
(61) Kobrak, M. N.; Znamenskiy, V. *Chem. Phys. Lett.* **2004**, *395*, 127–132.
(62) Shim, Y.; Duan, J.; Choi, M. Y.; Kim, H. J. *J. Chem. Phys.* **2003**, *119*, 6411–6414.
(63) De Andrade, J.; Böes, E. S.; Stassen, H. *J. Phys. Chem. B* **2002**, *106*, 3546.
(64) De Andrade, J.; Böes, E. S.; Stassen, H. *J. Phys. Chem. B* **2002**, *106*, 13344.
(65) Shah, J. K.; Brennecke, J. F.; Maginn, E. J. *Green Chem.* **2002**, *4*, 112–118.
(66) Margulis, C. J.; Stern, H. A.; Berne, B. J. *J. Phys. Chem. B* **2002**, *106*, 12017.
(67) Morrow, T. I.; Maginn, E. J. *J. Phys. Chem. B* **2002**, *106*, 12807.
(68) Hanke, C. G.; Price, S. L.; Lynden-Bell, R. M. *Mol. Phys.* **2001**, *99*, 801.
(69) Logotheti, G.-E.; Ramos, J.; Economou, I. G. *J. Phys. Chem. B* **2009**, *113*, 7211–7224.
(70) Micaelo, N. M.; Baptista, A. M.; Soares, C. M. *J. Phys. Chem. B* **2006**, *110*, 14444–14451.
(71) Lopes, J. C. N.; Pádua, A. A. H. *J. Phys. Chem. B* **2006**, *110*, 7485–7489.
(72) Tsuzuki, S.; Ayusawa Arai, A.; Nishikawa, K. *J. Phys. Chem. B* **2008**, *112*, 7739–7747.
(73) Tsuzuki, S.; Katoh, R.; Mikami, M. *Mol. Phys.* **2008**, *106*, 1621–1629.
(74) Katoh, R.; Hara, M.; Tsuzuki, S. *J. Phys. Chem. B* **2008**, *112*, 15426–15430.
(75) Hunt, P. A.; Gould, I. R. *J. Phys. Chem. A* **2006**, *110*, 2269–2282.
(76) Wang, Y.; Li, H.; Han, S. *J. Chem. Phys.* **2005**, *123*, 174501.
(77) Turner, E. A.; Pye, C. C.; Singer, R. D. *J. Phys. Chem. A* **2003**, *107*, 2277–2288.
(78) Kanakuboa, K.; Aizawa, T.; Nanjo, H.; Kameda, Y.; Amo, Y.; Usuki, T. Fluid Phase Equilib. [Online early access]. DOI: 10.1016/j.fluid.2010.03.043. Published Online: Apr 8, 2010.
(79) Gontrani, L.; Russina, O.; Lo Celso, F.; Caminiti, R.; Annat, G.; Triolo, A. *J. Phys. Chem. B* **2009**, *113*, 9235–9240.
(80) Kanakubo, M.; Ikeda, T.; Aizawa, T.; Nanjo, H.; Kameda, Y.; Amo, Y.; Usuki, T. *Anal. Sci.* **2008**, *24*, 1373–1376.
(81) Kanakubo, M.; Umecky, T.; Hiejima, Y.; Aizawa, T.; Nanjo, H.; Kameda, Y. *J. Phys. Chem. B* **2005**, *109*, 13847–13850.
(82) Hardacre, C.; Holbrey, J. D.; Mullan, C. L.; Nieuwenhuyzen, M.; Youngs, T. G. A.; Bowron, D. T. *J. Phys. Chem. B* **2008**, *112*, 8049–8056.
(83) Deetlefs, M.; Hardacre, C.; Nieuwenhuyzen, M.; Padua, A. A. H.; Sheppard, O.; Soper, A. K. *J. Phys. Chem. B* **2006**, *110*, 12055–12061.
(84) Deetlefs, M.; Hardacre, C.; Nieuwenhuyzen, M.; Sheppard, O.; Soper, A. K. *J. Phys. Chem. B* **2005**, *109*, 1593–1598.
(85) Hardacre, C.; Holbrey, J. D.; McMath, S. E. J.; Bowron, D. T.; Soper, A. K. *J. Chem. Phys.* **2003**, *118*, 273.
(86) Hardacre, C.; McMath, S. E. J.; Nieuwenhuyzen, M.; Bowron, D. T.; Soper, A. K. *J. Phys.: Condens. Matter* **2003**, *15*, S159–S166.
(87) Hagiwara, R.; Matsumoto, K.; Tsuda, T.; Ito, Y.; Kohara, S.; Suzuya, K.; Matsumoto, H.; Miyazaki, Y. *J. Non-Cryst. Solids* **2002**, *312*−*314*, 414–418.
(88) Takahashi, S.; Suzuya, K.; Kohara, S.; Koura, N.; Curuism, L. A.; Sabougni, M.-L. *Z. Phys. Chem.* **1999**, *209*, 209–221.
(89) Fujii, K.; Mitsugi, T.; Takamuku, T.; Yamaguchi, T.; Umebayashi, Y.; Ishiguro, S. *Chem. Lett.* **2009**, *38*, 340–341.
(90) Kanzaki, R.; Mitsugi, T.; Fukuda, S.; Fujii, K.; Takeuchi, M.; Soejima, Y.; Takamuku, T.; Yamaguchi, T.; Umebayashi, Y.; Ishiguro, S. *J. Mol. Liq.* **2009**, *147*, 77–82.
(91) Fukuda, S.; Takeuchi, M.; Fujii, K.; Kanzaki, R.; Takamuku, T.; Chiba, K.; Yamamoto, H.; Umebayashi, Y.; Ishiguro, S. *J. Mol. Liq.* **2008**, *148*, 2–7.
(92) Umebayashi, Y.; Chung, W.-L.; Mitsugi, T.; Fukuda, S.; Takeuchi, M.; Fujii, K.; Takamuku, T.; Kanzaki, R.; Ishiguro, S. *J. Comput. Chem., Jpn.* **2008**, *7*, 125–134.
(93) Fujii, K.; Soejima, Y.; Kyoshoin, Y.; Fukuda, S.; Kanzaki, R.; Umebayashi, Y.; Yamaguchi, T.; Ishiguro, S.; Takamuku, T. *J. Phys. Chem. B* **2008**, *112*, 4329–4336.
(94) Fujii, K.; Seki, S.; Fukuda, S.; Takamuku, T.; Kohara, S.; Kameda, Y.; Umebayashi, Y.; Ishiguro, S. *J. Mol. Liq.* **2008**, *143*, 64–69.
(95) Nockemann, P.; Binnemans, K.; Driesen, K. *Chem. Phys. Lett.* **2005**, *415*, 131.
(96) Earle, M. J.; Gordon, C. M.; Plechkova, N. V.; Seddon, K. R.; Welton, T. *Anal. Chem.* **2007**, *79*, 758.
(97) Burrel, A. R.; Del Sasto, R. E.; Baker, S. N.; McCleskey, T. M.; Baker, G. A. *Green Chem.* **2007**, *9*, 449.
(98) Umebayashi, Y.; Mori, S.; Fujii, K.; Tsuzuki, S.; Seki, S.; Hayamizu, K.; Ishiguro, S. *J. Phys. Chem. B* **2010**, *114*, 6513–6521.
(99) Umebayashi, Y.; Mitsugi, T.; Fujii, K.; Seki, S.; Chiba, K.; Yamamoto, H.; Lopes, J. N. C.; Pádua, A. A. H.; Takeuchi, M.; Kanzaki, R.; Ishiguro, S. *J. Phys. Chem. B* **2009**, *113*, 4338.
(100) Fujimori, T.; Fujii, K.; Kanzaki, R.; Chiba, K.; Yamamoto, H.; Umebayashi, Y.; Ishiguro, S. *J. Mol. Liq.* **2007**, *131*−*132*, 216–224.
(101) Asada, M.; Mitsugi, T.; Ogura, T.; Fujii, K.; Umebayashi, Y.; Ishiguro, S. *Anal. Sci.* **2007**, *23*, 835–840.
(102) Asada, M.; Mitsugi, T.; Fujii, K.; Kanzaki, R.; Umebayashi, Y.; Ishiguro, S. *J. Mol. Liq.* **2007**, *136*, 138–146.
(103) Fujii, K.; Kanzaki, R.; Takamuku, T.; Fujimori, T.; Umebayashi, Y.; Ishiguro, S. *J. Phys. Chem. B* **2006**, *110*, 8179.
(104) Umebayashi, Y.; Fujimori, T.; Sukizaki, T.; Asada, M.; Fujii, K.; Kanzaki, R.; Ishiguro, S. *J. Phys. Chem. A* **2005**, *109*, 8976–8982.
(105) Umebayashi, Y.; Mroz, B.; Asada, M.; Fujii, K.; Matsumoto, K.; Mune, Y.; Probst, M.; Ishiguro, S. *J. Phys. Chem. A* **2005**, *109*, 4862–4868.

(106) Zhang, Y.; Watanabe, N.; Miyawaki, Y.; Mune, Y.; Fujii, K.; Umebayashi, Y.; Ishiguro, S. *J. Solution Chem.* **2005**, *34*, 1429–1443.
(107) Umebayashi, Y.; Matsumoto, K.; Mune, Y.; Zhang, Y.; Ishiguro, S. *Phys. Chem. Chem. Phys.* **2003**, *5*, 2552–2556.
(108) Isshiki, M.; Ohishi, Y.; Goto, S.; Takeshita, K.; Takeshita, K.; Ishikawa, T. *Nucl. Instrum. Methods Phys. Res., Sect. A* **2001**, *467−468*, 663.
(109) Kohara, S.; Suzuya, K.; Kashihara, Y.; Matsumoto, N.; Umesaki, N.; Sakai, I. *Nucl. Instrum. Methods Phys. Res., Sect. A* **2001**, *467−468*, 1030.
(110) Sasaki, S. *KEK Report 90-16*; National Laboratory for High Energy Physics: Japan, 1991.
(111) Hubbell, J. H.; Veigele, W. J.; Briggs, E. A.; Brown, R. T.; Cromer, D. T.; Howerton, R. J. *J. Phys. Chem. Ref. Data* **1975**, *4*, 471.
(112) Cromer, D. T. *J. Chem. Phys.* **1969**, *50*, 4857.
(113) Cormer, D. T.; Mann, J. B. *J. Chem. Phys.* **1967**, *47*, 1892.
(114) Maslen, E. N.; Fox, A. G.; O'Keefe, M. A. *International Tables For Crystallography Vol. C*; Kluwer: Dordrecht, The Netherlands, 1999; pp 572−574.
(115) Johanson, G.; Sandstörm, M. *Chem. Scr.* **1973**, *4*, 195.
(116) Sambasivarao, S. V.; Acevedo, O. *J. Chem. Theory Comput.* **2009**, *5*, 1038–1050.
(117) Tsuzuki, S.; Shinoda, W.; Saito, H.; Mikami, M.; Tokuda, H.; Watanabe, M. *J. Phys. Chem. B* **2009**, *113*, 10641–10649.
(118) Köddermann, T.; Paschek, D.; Ludwig, R. *ChemPhysChem* **2008**, *9*, 549–555.
(119) Köddermann, T.; Paschek, D.; Ludwig, R. *ChemPhysChem* **2007**, *8*, 2464–2470.
(120) Zhao, W.; Eslami, H.; Cavalcanti, W. L.; Müller-Plathe, F. *Z. Phys. Chem.* **2007**, *221*, 1647–1662.
(121) Bhargavaa, B. L.; Balasubramanian, S. *J. Chem. Phys.* **2007**, *127*, 114510/1–114510/6.
(122) Wu, X.; Liu, Z.; Huang, S.; Wang, W. *Phys. Chem. Chem. Phys.* **2005**, *7*, 2771–2779.
(123) Lopes, J. N. C.; Deschamps, J.; Pádua, A. A. H. *J. Phys. Chem. B* **2004**, *108*, 2038–2047.
(124) Lopes, J. N. C.; Pádua, A. A. H. *J. Phys. Chem. B* **2004**, *108*, 16893–16898.
(125) Lopes, J. N. C.; Pádua, A. A. H. *J. Phys. Chem. B* **2006**, *110*, 19586–19592.
(126) Lopes, J. N. C.; Pádua, A. A. H.; Shimizu, K. *J. Phys. Chem. B* **2008**, *112*, 5039–5046.
(127) Tosi, M. P.; Fumi, G. *J. Phys. Chem. Solids* **1964**, *25*, 45.
(128) Jorgensen, W. L.; Maxwell, D. S.; Tirado-Rives, J. *J. Am. Chem. Soc.* **1996**, *118*, 11225.
(129) Kaminski, G.; Jorgensen, W. L. *J. Phys. Chem.* **1996**, *100*, 18010.
(130) Gear, G. W. *Numerical Initial Value Problems in Ordinary Differential Equations*; Prentice-Hall, Inc.: 1971.
(131) Berendsen, H. J. C.; Van Gunsteren, W. F. *Proceeding of the Enrico Fermi Summer School on Molecular dynamics simulation of statistical mechanical system*; Ciccotti, G., Hover, G., Ed.; North Holland: 1986; p 43.
(132) Nose, S. *Mol. Phys.* **1984**, *52*, 255.
(133) Nose, S. *J. Chem. Phys.* **1984**, *81*, 511.
(134) Parrinello, M.; Rahman, A. *J. Appl. Phys.* **1981**, *52*, 7182.
(135) Parrinello, M.; Rahman, A. *Phys. Rev. Lett.* **1980**, *45*, 1196.
(136) Broch-Carda, S.; Berthod, A.; Armstrong, D. W. *Anal. Bioanal. Chem.* **2003**, *375*, 191–199.
(137) Huddleston, J. G.; Visser, A. E.; Reichert, W. M.; Willauer, H. D.; Broker, G. A.; Rogers, R. D. *Green Chem.* **2001**, *3*, 156–164.
(138) Kim, K.-S.; Shin, B.-K.; Lee, H. *Korean J. Chem. Eng.* **2004**, *21*, 1010–1014.
(139) Frisch, M. J.; Trucks, G. W.; Schlegel, H. B.; Scuseria, G. E.; Robb, M. A.; Cheeseman, J. R.; Montgomery, J. A., Jr.; Vreven, T.; Kudin, K. N.; Burant, J. C.; Millam, J. M.; Iyengar, S. S.; Tomasi, J.; Barone, V.; Mennucci, B.; Cossi, M.; Scalmani, G.; Rega, N.; Petersson, G. A.; Nakatsuji, H.; Hada, M.; Ehara, M.; Toyota, K.; Fukuda, R.; Hasegawa, J.; Ishida, M.; Nakajima, T.; Honda, Y.; Kitao, O.; Nakai, H.; Klene, M.; Li, X.; Knox, J. E.; Hratchian, H. P.; Cross, J. B.; Bakken, V.; Adamo, C.; Jaramillo, J.; Gomperts, R.; Stratmann, R. E.; Yazyev, O.; Austin, A. J.; Cammi, R.; Pomelli, C.; Ochterski, J. W.; Ayala, P. Y.; Morokuma, K.; Voth, G. A.; Salvador, P.; Dannenberg, J. J.; Zakrzewski, V. G.; Dapprich, S.; Daniels, A. D.; Strain, M. C.; Farkas, O.; Malick, D. K.; Rabuck, A. D.; Raghavachari, K.; Foresman, J. B.; Ortiz, J. V.; Cui, Q.; Baboul, A. G.; Clifford, S.; Cioslowski, J.; Stefanov, B. B.; Liu, G.; Liashenko, A.; Piskorz, P.; Komaromi, I.; Martin, R. L.; Fox, D. J.; Keith, T.; Al-Laham, M. A.; Peng, C. Y.; Nanayakkara, A.; Challacombe, M.; Gill, P. M. W.; Johnson, B.; Chen, W.; Wong, M. W.; Gonzalez, C.; Pople, J. A. *Gaussian 03*, revision D.01; Gaussian, Inc.: Wallingford, CT, 2004.
(140) Godbout, N.; Salahub, D. R.; Andzelm, J.; Wimmer, E. *Can. J. Chem.* **1992**, *70*, 560.
(141) Shannon, R. D. *Acta Crystallogr.* **1976**, *A32*, 751.
(142) Urahata, S. M.; Ribeiro, M. C. C. *J. Chem. Phys.* **2004**, *120*, 1855–1863.
(143) Urahata, S. M.; Ribeiro, M. C. C. *J. Chem. Phys.* **2005**, *122*, 024511/1−024511/9.
(144) Urahata, S. M.; Ribeiro, M. C. C. *J. Chem. Phys.* **2006**, *123*, 074513/1−074513/8.
(145) Raabea, G.; Köhler, J. *J. Chem. Phys.* **2008**, *128*, 144503/1–144503/8.
(146) Raabea, G.; Köhler, J. *J. Chem. Phys.* **2008**, *128*, 154509/1−154509/7.
(147) Kowsari, M. H.; Alavi, S.; Ashrafizaadeh, M.; Najafi, B. *J. Chem. Phys.* **2008**, *129*, 224508/1–224508/13.
(148) Kowsari, M. H.; Alavi, S.; Ashrafizaadeh, M.; Najafi, B. *J. Chem. Phys.* **2009**, *130*, 014703/1−014703/10.
(149) Ando, R. A.; Siqueira, L. J. A.; Bazito, F. C.; Torresi, R. M.; Santos, P. S. *J. Phys. Chem. B* **2007**, *111*, 8717–8719.
(150) Schröder, C.; Rudas, T.; Steinhausera, O. *J. Chem. Phys.* **2006**, *125*, 244506/1–244506/10.
(151) Ghatee, M. H.; Ansari, Y. *J. Chem. Phys.* **2007**, *126*, 154502/1–154502/5.
(152) Qiao, B.; Krekeler, C.; Berger, R.; Site, L. D.; Holm, C. *J. Phys. Chem. B* **2008**, *112*, 1743–1751.
(153) Remsing, R. C.; Liu, Z.; Sergeyev, I.; Moyna, G. *J. Phys. Chem. B* **2008**, *112*, 7363–7369.
(154) Nakakoshi, M.; Shiro, M.; Fujimoto, T.; Machinami, T.; Seki, H.; Tashiro, M.; Nishikawa, K. *Chem. Lett.* **2006**, *35*, 1400–1401.

JP1044755